History-dependent control of unstable periodic orbits

P.M. Alsing,* A. Gavrielides,† and V. Kovanis‡
Nonlinear Optics Center, Phillips Laboratory,
3350 Aberdeen Avenue SE, Kirtland Air Force Base, New Mexico 87117-5776
(Received 18 March 1994)

We present a method of stabilizing unstable periodic orbits in systems whose natural time scales are on the order of or faster than the time it would take for the experimental implementation of the Ott-Grebogi-Yorke (OGY) controlling method [Phys. Rev. Lett. **64**, 1196 (1990)]. We determine the controlling perturbation one or more cycles ahead of when it needs to be applied, thereby gaining the additional time necessary to measure a signal, determine the perturbation, and then implement it. Formulas for this method of *prior iterate control* are derived and their utility is demonstrated numerically on the Hénon map for controlling the unstable orbits of period one and two. The effects of noise on this control method are examined and the results are compared with a similar application of the OGY scheme in the presence of noise.

PACS number(s): 05.45.+b

I. INTRODUCTION

With the publication of the seminal paper by Ott, Grebogi, and Yorke (OGY) [1] the concept of *controlling* chaos has become part of the lexicon of physicists and engineers dealing with chaotic nonlinear dynamical systems. The authors showed that by using small, judiciously applied perturbations the unstable periodic orbits, which are dense in a chaotic attractor, could be stabilized. The strength of their approach lies in the preclusion of the necessity for any *a priori* analytical model of the chaotic system in order to effect the control. The information required to construct the controlling perturbations can be extracted from experimental time series obtained from the unperturbed system. Since the publication of [1], the OGY controlling algorithm and numerous variations based upon its central concepts have been implemented numerically and experimentally in a host of nonlinear dynamical systems ranging from lasers and electronic circuits to chemical and biological systems. For excellent, recent review articles see [2] and the references therein.

The essence of the OGY algorithm is the astute observation that their are an infinte number of *unstable periodic orbits* buried in a chaotic attractor and they can be stabilized by applying conventional control theory techniques [3–5] to the (experimentally or numerically derived) Poincaré map of the dynamical system. By making the previously constant parameter time dependent, the dimension of the dynamical systems is raised by one and in this new dynamical system the old unstable periodic orbit is now stable and periodic. Since the appearance of [1] many theoretical refinements and modifications have been made to the OGY algorithm. In an accompanying article Ott, Grebogi, and Yorke [6] detailed how their basic algorithm for controlling the unstable period-one orbits presented in [1] could be extended to control unstable orbits of arbitrary period. Hunt [7] made a fast analog implementation of the OGY formula utilizing an occassional proportional feedback scheme. He successfully applied this method to control unstable periodic orbits of a driven diode resonator and, with Roy *et al.* [8], in a chaotic diode pumped solid-state laser system. Dressler and Nitsche [9] pointed out that with the use of a single scalar time series to construct an embedding of the attractor from delay coordinates, the OGY algorithm had to be slightly modified to include the effects of previous perturbations. In some cases, a parameter perturbation produces motion off the attractor leading to a singular OGY perturbation correction. Petrov *et al.* [10] and Rollins *et al.* [11] developed a modified control formula for such instances. The original formulation of the OGY algorithm uses the full set of phase space variables describing the dynamical system to effect the control. Auerbach *et al.* [12] have shown that control can be achieved by projecting down from the full set of phase space variables to a single time series. This method, which does not utilize a delay coordinate embedding, involves a history of the previous perturbations and is applicable to systems where the dimensions of the phase space is very high, possibly infinite. For the case of a nonlinear delay-differential dynamical system, which formally has an infinite-dimensional phase space, Gavrielides *et al.* [13] have presented a successful implementation of the OGY algorithm.

Schwartz and Triandaf [14] adapted the control scheme of OGY so that an unstable steady state could be tracked and stabilized over a wide range of values of the control parameter. With this method Gills *et al.* [15] were able to successfully increase the stable steady power output

*Electronic address: alsing@arom.plk.af.mil
†Electronic address: tom@photon.plk.af.mil
‡Also at Department of Mathematics and Statistics, University of New Mexico, Albuquerque, NM 87131. Electronic address: kovanis@xaos.plk.af.mil

of a laser by an order of magnitude. Bielawski *et al.* [16] were also able to track and control unstable periodic orbits over a range of values of the control parameter by of modification of the OGY algorithm. In their implementation, the controlling perturbation was proportional to the difference in the value of the signal at the present crossing of the surface of section and its value at the immediately preceding crossing. Mehta and Henderson [17] used the OGY algorithm to customize aperiodic orbits. Alsing *et al.* [18] demonstrated how neural networks could be used as chaotic controllers for a variety of OGY-based controlling formulas.

In the OGY algorithm, the control is effected through a parameter perturbation when the chaotic trajectory is in the neighborhood of the unstable periodic orbit. In contrast to this approach, stabilization of unstable periodic orbits can be achieved by the direct addition of feedback terms to the system. Efficient control has been obtained when the feedback is of the form of the difference between the present state of the system and the desired goal dynamics (for futher details see references in [2]). The method could be called *dissipative control* in the sense that the feedback terms introduce a damping term in the equations for the linearized error signal between the system and the goal dynamics. In many cases there is a range of values for the damping term in which the linearized error signal is driven to zero, thus bringing the system to the desired orbit.

Pyragas [19] has recently formulated an interesting variation of this feedback control. In his scheme, the feedback term is proportional to the difference between the present state of the system and the state of the system one period earlier. This control scheme is a form of autosynchronization which stabilizes the unstable period-one orbit. Socolar and co-workers [20] have proposed an extension of this method of control via autosynchronization, which involves a weighted sum of the signal at all previous multiples of the period. Such a scheme could be implemented optically and find potential use in stabilizing unstable periodic orbits in optical systems where the time scales are very fast.

The advantage of these dissipative control schemes is that they can be implemented continuously, as opposed to the OGY scheme where control is implemented intermitantly when the trajectory crosses a surface of section. This can be a definite advantage when it comes to practically implementing the controlling scheme. A disadvantage of the dissipative control schemes, albeit of a more theoretical than practical nature, is that the range of values for the proportionality constant of the feedback term which produces control cannot, in general, be determined *a priori*. One must either find them by direct experimentation or, if a model of the dynamical system equations exists, numerically determine them from a calculation of the Lyapunov spectrum. The extension of this scheme for stabilizing oribits in high dimensional attractors is therefore not as conceptually straightforward as the OGY method. With respect to this problem the work of So *et al.* [21], who extended the control theory concept of a state observer to nonlinear chaotic systems, may find applicability.

In most experimental implementations of the OGY scheme (including its variants) the natural time scales of the systems have been below 100 kHz [7,8,22]. Therefore experimentalists have not been overly concerned with the time involved in the process of detecting the signal at some crossing of a surface of section, calculating the required perturbation, and then applying that perturbation. If this processing time is on the order of the natural time scale for the dynamical system, such as in optical or semiconductor devices, the implementation of the OGY algorithm becomes problematic. In this respect, the features of the continuous controlling schemes described above could prove advantageous for low-dimensional attractors.

In this paper we are concerned with addressing this problem of controlling the unstable periodic orbits in systems whose natural times scales are on the order of or faster than the time it would take to measure the signal and implement the standard OGY controlling formula. In order to extend the applicability of the OGY scheme to such systems with fast time scales, we present a controlling scheme which utilizes information from a prior sampling of the signal to stablize the unstable periodic orbit. We determine the required peturbation one or more cycles ahead of when it needs to be applied, thereby purchasing the time necessary to measure the signal, determine the perturbation, and then implement it.

The organization of this paper is as follows. In Sec. II we derive this method of *prior iterate control* (PIC) in a iterative fashion from the standard OGY formula. We derive the PIC formula utlizing information one iterate back from the present signal measurement and then generalize the formula to one using an arbitrary number of iterates back. A numerical demonstration of the PIC formulas is given for the Hénon map. We also investigate the effects of noise on the PIC method and compare the results to a similar application of the OGY scheme in the presence of noise. In Sec. III we discuss the generalization of this scheme to the problem of controlling higher periodic orbits. We give explicit formulas for period-two orbits and again demonstrate the algorithm on the Hénon map. After stating our conclusions, we present two appendixes. In Appendix A we develop the PIC formula corresponding to the Dressler-Nitsche modification of the OGY formula when delay coordinates are involved. In Appendix B we relate the OGY and PIC algorithms to the problem of pole placement in conventional control theory.

II. THE OGY FORMULA AND PRIOR ITERATE CONTROL METHODS

A. Derivation of formulas

Let us begin by first recalling the derivation of the now standard OGY controlling formula. For simplicity, we assume that the chaotic map has one positive Lyapunov exponent. Suppose we have a mapping $\boldsymbol{\xi}_{n+1} = \boldsymbol{F}(\boldsymbol{\xi}_n, p)$, where $\boldsymbol{\xi}_n$ is a vector of the phase space variables and p is a parameter whose nominal value is p_0. The linearized map $\boldsymbol{\xi}_{n+1} - \boldsymbol{\xi}_F(p) = \boldsymbol{M}\,[\boldsymbol{\xi}_n - \boldsymbol{\xi}_F(p)]$ governs the evolution of small peturbations about the parameter-dependent fixed point $\boldsymbol{\xi}_F(p)$ in the neighborhood of the unstable fixed point $\boldsymbol{\xi}_F(p_0)$ of the unperturbed map. Here $\boldsymbol{M} \equiv \boldsymbol{D}_{\xi}\boldsymbol{F}(\boldsymbol{\xi}_F(p_0), p_0)$ is the Jacobian of the map $\boldsymbol{F}$ evaluated at the fixed point $\boldsymbol{\xi}_F(p_0)$ and the nominal parameter value p_0. For small perturbations of p about p_0, the perturbed fixed point can be expressed in terms of the unperturbed fixed point as $\boldsymbol{\xi}_F(p) = \boldsymbol{\xi}_F(p_0) + \boldsymbol{\Delta}\delta p_n$, where we have defined $\boldsymbol{\Delta} \equiv \partial\boldsymbol{\xi}_F(p_0)/\partial p$. Defining $\delta\boldsymbol{\xi}_n \equiv \boldsymbol{\xi}_n - \boldsymbol{\xi}_F(p_0)$ enables the local mapping to be written as

$$\delta\boldsymbol{\xi}_{n+1} = \boldsymbol{M}\,\boldsymbol{\xi}_n + (1 - \boldsymbol{M})\,\boldsymbol{\Delta}\,\delta p_n. \tag{2.1}$$

Control of the unstable period-one orbit is obtained by requiring that $\boldsymbol{\xi}_{n+1}$ has no projection on the unstable manifold. This can be written as $\boldsymbol{f}_u \cdot \boldsymbol{\xi}_{n+1} = 0$, where $\boldsymbol{f}_u$ is the unstable contravariant (left) eigenvector of $\boldsymbol{M}$ with eigenvalue λ_u ($|\lambda_u| > 1$), $\boldsymbol{f}_u\,\boldsymbol{M} = \lambda_u\,\boldsymbol{f}_u$. The OGY control formula is then given by [1]

$$\delta p_n = \frac{\lambda_u}{\lambda_u - 1}\frac{\boldsymbol{f}_u \cdot \delta\boldsymbol{\xi}_n}{\boldsymbol{f}_u \cdot \boldsymbol{\Delta}}. \tag{2.2}$$

The OGY formula Eq. (2.2) entails a measurement of the signal difference $\boldsymbol{\xi}_n - \boldsymbol{\xi}_F(p_0)$ at the nth iteration of the map, the construction of δp_n, and the immediate application of this perturbation in order to effect a change in $\boldsymbol{\xi}_{n+1} - \boldsymbol{\xi}_F(p_0)$, the signal difference at the next iterate. In most experimental applications of the OGY formula, the combined time involved in the process of signal detection, calculation of the pertubation, and its subsequent application has been negligible compared to the average time between successive iterate crossings of the surface of section. This is because the intrinsic time scale of most of the experimental applications has been long compared with the time scale for which fast electronics can implement the control. However, as the intrinsic time scale of the system approaches the time scale on which control can be effected, the implementation of the standard OGY method, or even fast analog variants such as Hunt's occasional proportional feedback scheme, becomes problematic. Such situtations can occur in semiconductor lasers operating at gigahertz frequencies [13], antireflection coated semiconductor laser in an external cavity operating around 100 MHz [23], and ultrafast electronic circuits [19,20].

The question then becomes whether one can use the data from iterates prior to the nth to control the $n+1$ iterate. We can accomplish this by writing down Eq. (2.1) for the n iterate $\delta\boldsymbol{\xi}_n = \boldsymbol{M}\,\boldsymbol{\xi}_{n-1} + (1 - \boldsymbol{M})\,\boldsymbol{\Delta}\,\delta p_{n-1}$ and substituting this back into Eq. (2.1). Requiring once again that $\boldsymbol{f}_u \cdot \boldsymbol{\xi}_{n+1} = 0$ yields

$$\delta p_n^{(1)} = \lambda_u \left[-\delta p_{n-1}^{(1)} + \frac{\lambda_u}{\lambda_u - 1}\frac{\boldsymbol{f}_u \cdot \delta\boldsymbol{\xi}_{n-1}}{\boldsymbol{f}_u \cdot \boldsymbol{\Delta}}\right]. \tag{2.3}$$

Equation (2.3) embodies the central features of the PIC method and is the main mathematical result of this paper.

Equation (2.3) has a form reminiscent to that of the control formula of Dressler and Nitsche [9]; however, the two are very different. The Dressler-Nitsche formula arose in the context of using delay coordinates, which produced a dependence of δp_n on δp_{n-1}. In addition, the Dressler-Nitsche formula uses the signal difference $\delta\boldsymbol{\xi}_n$ at the nth iterate as opposed to Eq. (2.3), which uses the signal difference $\delta\boldsymbol{\xi}_{n-1}$ at the $n-1$ iterate. The procedure of using information "one iterate back" to effect the control is signified by the superscript (1) on the δp_n's in Eq. (2.3) and is the justification for calling this procedure *prior iterate control.* In Appendix A we present the PIC formula analogous to Eq. (2.3), which applies to the Dressler-Nitsche modification of the OGY formula.

For purposes of explanation, we may think of our Poincaré surface of section as being defined as the peaks of the signal of one of the phase space variables $\xi_k \in \boldsymbol{\xi}$ (i.e., $\dot{\xi}_k = 0$, $\ddot{\xi}_k < 0$). The OGY formula Eq. (2.2) uses information obtained at the nth peak to control the height of the $n+1$ peak. Implicit in this scheme is the assumption that the total time to detect the signal peak, calculate the perturbation, and apply the control Δt_n is much less than the time between peaks $t_{n+1} - t_n$, i.e., the time between consecutive crossings of a surface of section. In contrast, the PIC formula Eq. (2.3) uses information obtained one peak back, at $n-1$, and the previous pertubation in order to accomplish the same task. This is schematically illustrated in Fig. 1 for a generic scalar time series. The cost incurred in using information one peak back to implement control is manifest in the extra factor of λ_u, which appears out front in Eq. (2.3), arising from the use of $\boldsymbol{M}^2$ in going from $\delta\boldsymbol{\xi}_{n-1}$ to $\delta\boldsymbol{\xi}_{n+1}$. An equivalent way to view Eq. (2.3) is as follows. Iterating the indices one step forward, Eq. (2.3) gives $\delta p_{n+1}^{(1)} = \lambda_u\,[-\delta p_n^{(1)} + (\lambda_u\,\boldsymbol{f}_u \cdot \delta\boldsymbol{\xi}_n)/(\lambda_u - 1)\,\boldsymbol{f}_u \cdot \boldsymbol{\Delta}]$. At the nth iterate we have the detected signal difference $\delta\boldsymbol{\xi}_n$ and apply the perturbation $\delta p_n^{(1)}$, which has been calculated from the previous signal diffence $\delta\boldsymbol{\xi}_{n-1}$. Therefore, we have all the necessary information to calculate $\delta p_{n+1}^{(1)}$ at the nth iterate. The calculated $\delta p_{n+1}^{(1)}$ is then held to the next iterate at time t_{n+1}, where it is implemented to stabilize the next peak x_{n+2} (see Fig. 1).

One notes that Eq. (2.3) is self-consistent in the sense that when $\delta p_n^{(1)}$ approaches zero, the right-hand side reproduces the OGY formula for control one iterate back at the $n-1$ peak. The OGY formula Eq. (2.2) can be considered as the particular pole placement solution of conventional control theory [4], applied to the Poincaré map about the fixed point (i.e., with the discrete state space vector $\boldsymbol{x}_n = \delta\boldsymbol{\xi}_n$), which locally replaces the unstable eigenvalue λ_u with zero and leaves the stable eigenvalues unchanged [3]. In the same way, Eq. (2.3) is the analogous pole placement solution for the enlarged state space $\boldsymbol{x}'_n = \{\delta\boldsymbol{\xi}_n, \delta p_n^{(1)}\}$ (see Appendix B).

We can extend the above result to the case of using $\delta\boldsymbol{\xi}_{n-k}$ to control the $n+1$ peak by deriving a formula for $\delta p_n^{(k)}$ in a manner similar to the derivation of Eq. (2.3),

$$\delta p_n^{(k)} = \lambda_u \left[-\delta p_{n-1}^{(k)} + \lambda_u \left[-\delta p_{n-2}^{(k)} + \lambda_u \left[\cdots + \lambda_u \left[-\delta p_{n-k}^{(k)} + \frac{\lambda_u}{\lambda_u - 1} \frac{\boldsymbol{f}_u \cdot \delta \boldsymbol{\xi}_{n-k}}{\boldsymbol{f}_u \cdot \boldsymbol{\Delta}} \right] \cdots \right] \right] \right]. \tag{2.4}$$

Again we see that when $\delta p_n^{(k)} = 0$ the central bracket on the right-hand side of Eq. (2.4) reproduces the OGY formula for the iterate $n-k$. Figure 2 shows a comparison of Eqs. (2.2) and (2.4) applied to the Hénon map for $k = \{0, 1, 4, 5\}$. Note that for $k = 0$, $\delta p^{(0)}$ is given by the OGY formula Eq. (2.2). In both instances the perturbations are constructed from the local map $\boldsymbol{M}$, which is obtained from a numerical fit of data taken about the fixed point.

Equivalently, we can view Eq. (2.4) as follows. At the nth iterate we have the signal difference $\delta \boldsymbol{\xi}_n$ and apply the perturbation $\delta p_n^{(k)}$, which has been previously calculated using the signal difference $\delta \boldsymbol{\xi}_{n-k}$. By shifting the indices of Eq. (2.4) from $n \to \{n+1, n+2, \ldots, n+k\}$, we have all the necessary information to calculate $\{\delta p_{n+1}^{(k)}, \delta p_{n+2}^{(k)}, \ldots, \delta p_{n+k}^{(k)}\}$ at the nth iterate. By keeping a history of the $\delta \boldsymbol{\xi}_n$ and $\delta p_n^{(k)}$ used, we can always maintain a time interval corresponding to k iterations (i.e., $t_n - t_{n-k}$), between the time at which we compute the perturbation and the time when we need to apply it.

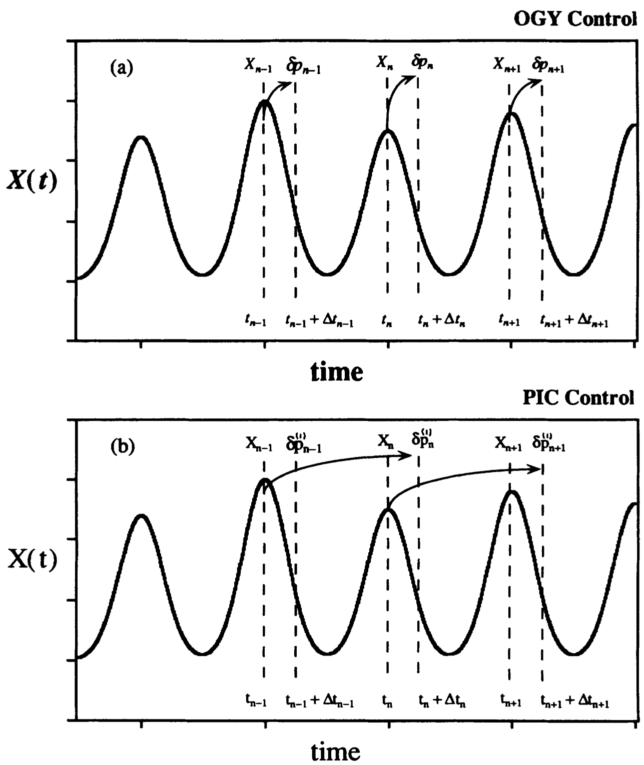

FIG. 1. Implementation of the OGY and PIC controlling scheme to a generic scalar time series. (a) In the OGY controlling scheme, a signal x_n is measured at time t_n. The perturbation δp_n is calculated and then applied a short instant later at time $t_n + \Delta t_n$. The implicit assumption used here is that the time between consecutive peaks $t_{n+1} - t_n$ is much longer than the time to implement the control Δt_n. (b) In the PIC controlling scheme, the signal is again measured at time t_n. With these data the perturbation $\delta p_{n+1}^{(1)}$ can be calculated and held until it is applied at $t_{n+1} + \Delta t_{n+1}$, after the measurement of x_{n+1}. Note that at time $t_n + \Delta t_n$, the perturbation $\delta p_n^{(1)}$, which was previously calculated one iterate back at x_{n-1}, is being applied.

B. Controlling in the presence of noise

At this point one might be concerned with the validity of iterating a linear approximation of the local map Eq. (2.1) an arbitrary number of times without worrying about higher-order correction terms. Since the PIC formulas Eq. (2.4) are valid pole placement solutions to the control problem (see Appendix B) and are linear in the deviation vector $\delta \boldsymbol{\xi}_{n-k}$, the region of control must be smaller than that for Eq. (2.1) in order for the linear approximation to hold. We can see this as follows. OGY defined an effective region of control [1] for a given maximum allowable perturbation $\delta p_{\max}$ as $|\xi_n^u| < \xi_*^{(0)}$, where $\xi_n^u \equiv \boldsymbol{f}_u \cdot \boldsymbol{\xi}_n$ and

$$\xi_*^{(0)} = \delta p_{\max} |(1 - \lambda_u^{-1}) \boldsymbol{f}_u \cdot \boldsymbol{\Delta}|. \tag{2.5}$$

We now consider the PIC formula Eq. (2.4) when control is just beginning to be initiated. At this point in time $\delta p_{n-i}^{(k)} = 0$ for $i = 1, 2, \ldots, k$ and Eq. (2.4) reads $\delta p_n^{(k)} = \lambda_u^k (\lambda_u \boldsymbol{f}_u \cdot \delta \boldsymbol{\xi}_{n-k}) / [(\lambda_u - 1) \boldsymbol{f}_u \cdot \boldsymbol{\Delta}]$. If we keep the same maximum perturbation $\delta p_{\max}$ we can derive a formula for $\xi_*^{(k)}$ in analogy with that for the OGY radius $\xi_*^{(0)}$ given above. We find

$$\xi_*^{(k)} = |\lambda_u|^{-k} \xi_*^{(0)}. \tag{2.6}$$

Thus the initial region of control for Eq. (2.4) is $|\lambda_u|^k$ times smaller than for the original OGY formula Eq. (2.2). Equation (2.6) states that the use of the prior iterates $\delta \boldsymbol{\xi}_{n-k}$ to implement control requires the trajectories be $|\lambda_u|^k$ closer to the fixed point in order for the PIC formula to lock on and stabilize the orbit. This is schematically illustrated in Fig. 3. Equivalently, one may interpret Eq. (2.6) as follows. Suppose that at the $n-k$ iterate, the PIC algorithm is implemented over a region $\xi_*^{(k)}$ given by Eq. (2.6). After k iterates the trajectory could have diverged by at most a factor of $|\lambda_u|^k$. Therefore, the trajectory at the nth iterate will still be contained in the region of size $\xi_*^{(0)}$, applicable to the standard OGY algorithm.

The smaller region $\xi_*^{(k)}$, over which stabilization can be achieved, validates the use of a linear approximation Eq. (2.4) for the control formula over this region. In general, one may be satisfied with having the largest possible control region, for a given maximum allowable perturbation, as given by the OGY formula Eq. (2.2). However, if one needs time on the order of the duration between successive peaks of the signal in order to implement the

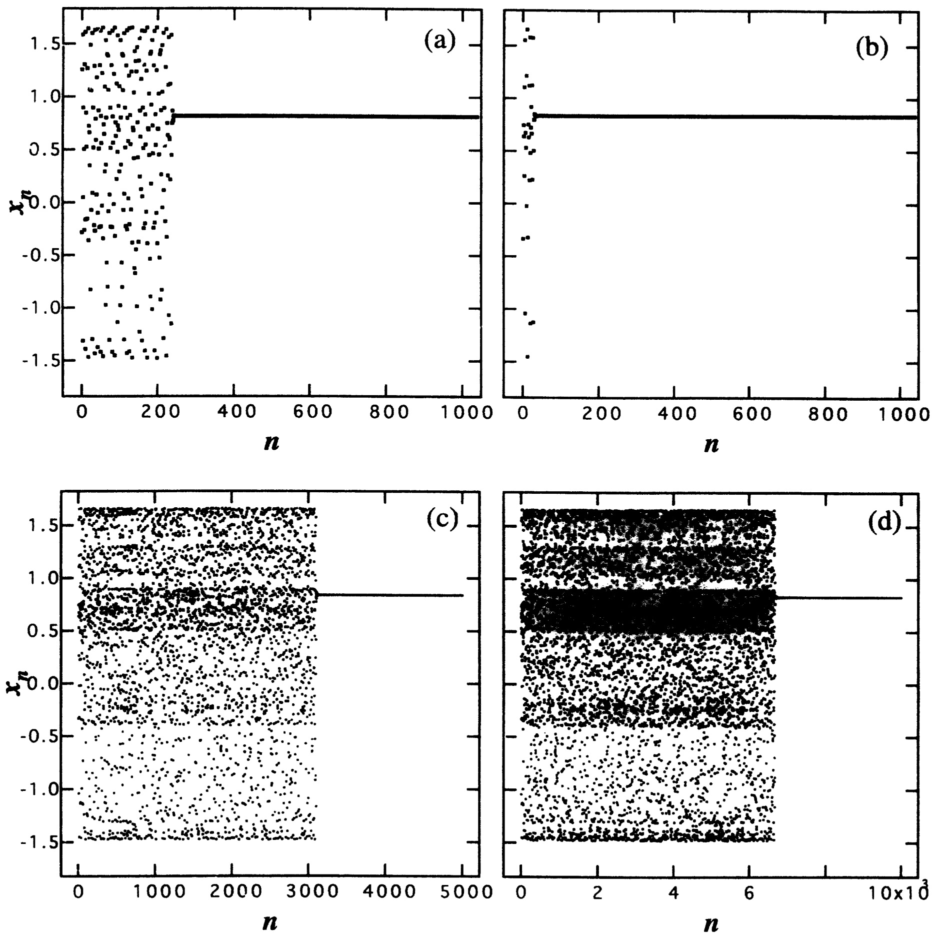

FIG. 2. Controlling the unstable period-one orbit of the Hénon map using the PIC algorithm Eq. (2.4), for k iterates back: (a) $k = 0$, (b) $k = 1$, (c) $k = 4$, and (d) $k = 5$. Note that $k = 0$ corresponds to the OGY formula, Eq. (2.2).

controlling algorithm, the PIC formula states that this can be achieved at the sacrifice of having a smaller region over which control can be initiated. This also implies that the time for the control algorithm to stabilize the unstable periodic orbit will increase as $\xi_*^{(k)}$ decreases.

In their original paper, OGY [1] examined the validity of Eq. (2.5) by adding noise of the form $\epsilon\boldsymbol{\delta}_n$ to the right-hand side of the Hénon map equations $x_{n+1} = A + \delta p_n - x_n^2 + B\,y_n,\ y_{n+1} = x_n$, with $A = 1.29$ and $B = 0.3$. Here $\boldsymbol{\delta}_n$ was taken to be a zero mean, unit variance Gaussian random variable and δp_* was held fixed at $\delta p_* = 0.2$. For bounded noise, i.e., $|\delta_n^u \equiv \boldsymbol{f}_u \cdot \boldsymbol{\delta}_n| < \delta_{\max}$ for some fixed $\delta_{\max}$, control was lost when $\epsilon\delta_{\max} > \xi_*^{(0)}$.

Similary, we can test the validity of the PIC controlling region Eq. (2.6) by examining its tolerance to noise for different values of k. To account for the dependence of the chaotic transient preceeding control on $\delta p_{\max}$ [1], we scaled the maximum perturbation $\delta p_{\max}^{(k)}$ for a given $k \le k_{\max}$ via $\delta p_{\max}^{(k)} = \delta p_{\max}\,|\lambda_u|^k/|\lambda_u|^{k_{\max}}$. For a given k the Hénon map was iterated under noise-free conditions until the unstable period-one orbit was controlled using the usual OGY algorithm Eq. (2.2). After the orbit was stabilized for an arbitrary length of time, Gaussian noise $\epsilon^{(k)}\boldsymbol{\delta}_n$ was added to the equations, as described above, and the maximum allowable perturbation was set to $\delta p_{\max}^{(k)}$ using $\delta p_{\max} = 0.2$. Iterations proceeded for a fixed length of time. The system was deemed partially controlled if a fixed number of consecutive iterates (~ 10) remained within a predefined narrow band about the fixed point. If this was not the case, the system was deemed uncontrolled. For each run we measured the ratio of the time the system was partially controlled to the total time control was attempted.

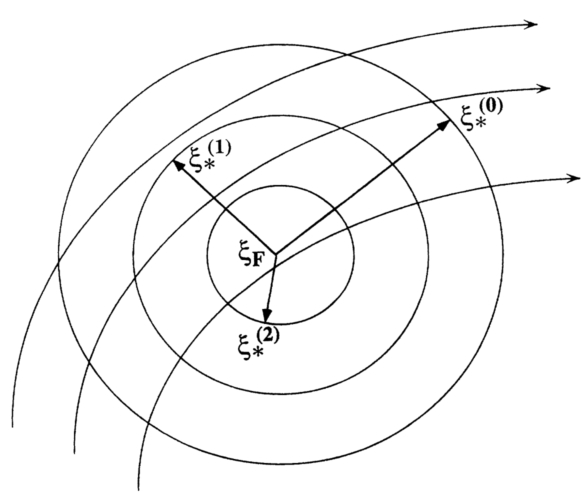

FIG. 3. The controlling region $\boldsymbol{\xi}_*^{(k)}$ for the PIC algorithm using data k iterates back (i.e., $\delta\boldsymbol{\xi}_{n-k}$) is $|\lambda_u|^{(k)}$ smaller than the corresponding control region $\boldsymbol{\xi}_*^{(0)}$ for the OGY algorithm.

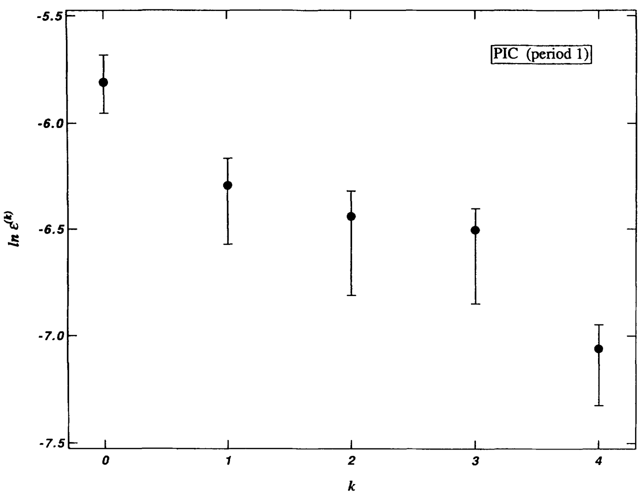

FIG. 4. Plot of $\ln \epsilon^{(k)}$ vs k for the unstable period-one orbit of the Hénon map using the PIC algorithm Eq. (2.4), for $k = \{0,1,2,3,4\}$ iterates back. $\epsilon^{(k)}$ is the magnitude of the Gaussian noise added to the Hénon map at which control, using the PIC algorithm for k iterates back, is 95% lost.

For each k at least 200 runs were performed in order to build up statistics. A mean value of $\epsilon^{(k)}$ was searched for in which the above ratio of the (time partially controlled)/(total time control was attempted) was 5%. For different values of k this let us test the hypothesis that $\epsilon^{(k)}[5\%]\,\delta_{\max} \sim \xi_*^{(k)} = |\lambda_u|^{-k}\xi_*^{(0)}$, where Eq. (2.6) was used in the last equality. In Fig. 4 we have plotted the results of $\ln \epsilon^{(k)}[5\%]$ versus k, where $k_{\max} = 4$. The central points are the mean of $\ln \epsilon^{(k)}[5\%]$ and the extreme points of the error bars indicate plus and minus one standard deviation. The exponential of the negative of the slope yields a mean value of $|\lambda_u| \sim 1.33$, which is somewhat smaller than the true value of $|\lambda_u| = 1.84$. This exercise qualitatively shows that Eq. (2.6) is valid, which implies that the region of control shrinks by a factor of $|\lambda_u|$ for each prior iterate for purpose of control. The discrepancies between the computed and the exact values of $|\lambda_u|$ are most likely due to the imprecise scaling of $\delta p_{\max}^{(k)}$ in order to take into account the longer duration of the chaotic transient for smaller values of the maximum allowable perturbation.

III. CONTROLLING HIGHER-ORDER UNSTABLE PERIODIC ORBITS

In a subsequent paper [6] Ott, Grebogi, and Yorke describe how to control unstable periodic orbits of arbitrary period. For means of illustration we discuss both the OGY formula and the PIC scheme for period-two orbits. Taking again our surface of section to be the peaks of our temporal signal, an unstable period-two orbit would be described by consecutive pairs of high and low peaks corresponding to the two unstable fixed points of the map $\boldsymbol{\xi}_F^{(1)}(p_0)$ and $\boldsymbol{\xi}_F^{(2)}(p_0)$. There are then two local mappings of interest: one from the neighborhood of $\boldsymbol{\xi}_F^{(1)}(p_0)$ to $\boldsymbol{\xi}_F^{(2)}(p_0)$ given by $\boldsymbol{M}_1$ (say the high peak to the low peak) and from the neighborhood of $\boldsymbol{\xi}_F^{(2)}(p_0)$ back to $\boldsymbol{\xi}_F^{(1)}(p_0)$ given by $\boldsymbol{M}_2$ (the low peak back to the high peak). This is illustrated schematically in Fig. 5.

In analogy with Eq. (2.1) we can write the local mappings as

$$\begin{aligned}\boldsymbol{\xi}_{n+1} - \boldsymbol{\xi}_F^{(2)}(p_0) &= \boldsymbol{M}_1\,[\boldsymbol{\xi}_n - \boldsymbol{\xi}_F^{(1)}(p_0)] \\ &\quad +[\boldsymbol{\Delta}^{(2)} - \boldsymbol{M}_1\,\boldsymbol{\Delta}^{(1)}]\,\delta p_n, \qquad (3.1)\\ \boldsymbol{\xi}_{n+2} - \boldsymbol{\xi}_F^{(1)}(p_0) &= \boldsymbol{M}_2\,[\boldsymbol{\xi}_{n+1} - \boldsymbol{\xi}_F^{(2)}(p_0)] \\ &\quad +[\boldsymbol{\Delta}^{(1)} - \boldsymbol{M}_2\,\boldsymbol{\Delta}^{(2)}]\,\delta p_{n+1}, \qquad (3.2)\end{aligned}$$

where we have defined $\boldsymbol{\Delta}^{(i)} \equiv \partial\boldsymbol{\xi}_F^{(i)}(p_0)/\partial p$, $i = \{1,2\}$. As a specific example, for two-dimensional maps with one unstable and one stable eigendirection we would have $\boldsymbol{M}_1 = \lambda_u^{(1)}\boldsymbol{e}_u^{(2)}\boldsymbol{f}_u^{(1)} + \lambda_s^{(1)}\boldsymbol{e}_s^{(2)}\boldsymbol{f}_s^{(1)}$ and $\boldsymbol{M}_2 = \lambda_u^{(2)}\boldsymbol{e}_u^{(1)}\boldsymbol{f}_u^{(2)} + \lambda_s^{(2)}\boldsymbol{e}_s^{(1)}\boldsymbol{f}_s^{(2)}$, where $\boldsymbol{e}_{s,u}^{(i)}$ and $\boldsymbol{f}_{s,u}^{(i)}$ are the stable and unstable eigenvectors and contravariant eigenvectors, respectively, at the fixed point $\boldsymbol{\xi}_F^{(i)}(p_0)$ satisfying $\boldsymbol{f}_{s,u}^{(i)} \cdot \boldsymbol{e}_{s,u}^{(i)} = 1$ and $\boldsymbol{f}_{s,u}^{(i)} \cdot \boldsymbol{e}_{u,s}^{(i)} = 0$. Control is achieved by projecting the left-hand sides of Eqs. (3.1) and (3.2) off the appropriate unstable directions, i.e., requiring $\boldsymbol{f}_u^{(2)}\cdot[\boldsymbol{\xi}_{n+1} - \boldsymbol{\xi}_F^{(2)}(p_0)] = 0$ and $\boldsymbol{f}_u^{(1)}\cdot[\boldsymbol{\xi}_{n+2} - \boldsymbol{\xi}_F^{(1)}(p_0)] = 0$. This produces the perturbations

$$\delta p_n = \frac{\lambda_u^{(1)}\boldsymbol{f}_u^{(1)}\cdot[\boldsymbol{\xi}_n - \boldsymbol{\xi}_F^{(1)}(p_0)]}{\lambda_u^{(1)}\boldsymbol{f}_u^{(1)}\cdot\boldsymbol{\Delta}^{(1)} - \boldsymbol{f}_u^{(2)}\cdot\boldsymbol{\Delta}^{(2)}}, \qquad (3.3)$$

$$\delta p_{n+1} = \frac{\lambda_u^{(2)}\boldsymbol{f}_u^{(2)}\cdot[\boldsymbol{\xi}_{n+1} - \boldsymbol{\xi}_F^{(2)}(p_0)]}{\lambda_u^{(2)}\boldsymbol{f}_u^{(2)}\cdot\boldsymbol{\Delta}^{(2)} - \boldsymbol{f}_u^{(1)}\cdot\boldsymbol{\Delta}^{(1)}}. \qquad (3.4)$$

Equation (3.3) is the OGY perturbation implemented in going from the high peak to the low peak and Eq. (3.4) is the OGY perturbation implemented in going from the low peak back to the high peak.

In practical application to many low-dimensional mappings, one can often avoid the use of two explicit mappings and instead invoke a local mapping derived from

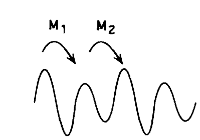

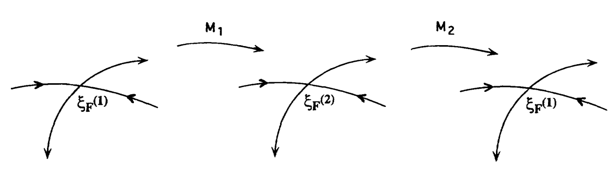

FIG. 5. The mappings $\boldsymbol{M}_1$ and $\boldsymbol{M}_2$ for the unstable period-two orbit of the Hénon map. The fixed points $\boldsymbol{\xi}_F^{(1)}$ and $\boldsymbol{\xi}_F^{(2)}$ can be thought of as the high and low peak, respectively, of the period-two orbit. $\boldsymbol{M}_1$ is then the map from the high peak to the low peak and $\boldsymbol{M}_2$ is the map from the low peak back to the high peak.

a surface of section defined by say only the high peaks or only the low peaks. The former would be a direct mapping from $\boldsymbol{\xi}_n - \boldsymbol{\xi}_F^{(1)}(p_0)$ to $\boldsymbol{\xi}_{n+2} - \boldsymbol{\xi}_F^{(1)}(p_0)$ via the composite map $\boldsymbol{M}_2\boldsymbol{M}_1$ and the latter would be a direct mapping from $\boldsymbol{\xi}_n - \boldsymbol{\xi}_F^{(2)}(p_0)$ to $\boldsymbol{\xi}_{n+2} - \boldsymbol{\xi}_F^{(2)}(p_0)$ via the composite map $\boldsymbol{M}_1\boldsymbol{M}_2$. In the case of PIC applied to unstable period-two orbits, we found that such squared mappings from one fixed point back to itself did not work. We found that we had to use the two separate forms of perturbations for the transition from one fixed point to the other and then for the transition back again.

The derivation of the PIC formula for unstable period-two orbits for $k = 1$ (one iterate back) proceeds as follows. We change indices $n \to n-2$ in Eq. (3.2), substitute this result into the right-hand side of Eq. (3.1), and set the projection of this resulting equation onto $\boldsymbol{f}_u^{(2)}$ equal to zero. This produces the perturbation $\delta p_n^{(1)}$. Similarly, to produce $\delta p_{n+1}^{(1)}$ we substitute Eq. (3.1) into the right-hand side of Eq. (3.2) and set the projection of this resulting equation onto $\boldsymbol{f}_u^{(1)}$ equal to zero. The forms of these perturbations are given by

$$\delta p_n^{(1)} = \frac{\lambda_u^{(1)}}{D^{(1)}} \{ -D^{(2)}\, \delta p_{n-1}^{(1)} + \lambda_u^{(2)}\, \boldsymbol{f}_u^{(2)} \cdot [\boldsymbol{\xi}_{n-1} - \boldsymbol{\xi}_F^{(2)}(p_0)] \}, \tag{3.5a}$$

$$\delta p_{n+1}^{(1)} = \frac{\lambda_u^{(2)}}{D^{(2)}} \{ -D^{(1)}\, \delta p_n^{(1)} + \lambda_u^{(1)}\, \boldsymbol{f}_u^{(1)} \cdot [\boldsymbol{\xi}_n - \boldsymbol{\xi}_F^{(1)}(p_0)] \}, \tag{3.5b}$$

where we have defined $D^{(1)} \equiv \lambda_u^{(1)} \boldsymbol{f}_u^{(1)} \cdot \boldsymbol{\Delta}^{(1)} - \boldsymbol{f}_u^{(2)} \cdot \boldsymbol{\Delta}^{(2)}$ and $D^{(2)} \equiv \lambda_u^{(2)} \boldsymbol{f}_u^{(2)} \cdot \boldsymbol{\Delta}^{(2)} - \boldsymbol{f}_u^{(1)} \cdot \boldsymbol{\Delta}^{(1)}$. Prior iterate control is seen in above formulas by the fact that $\delta p_n^{(1)}$ utilizes information from the $n-1$ peak as opposed to the nth peak, and similary $\delta p_{n+1}^{(1)}$ uses information one peak back.

The generalization of Eq. (3.5) for PIC using information k iterates back is straightforward, but notationally cumbersome. It is useful to introduce the symbol $\mathcal{R}_2(k) \equiv$ [the remainder of $(k/2)$ mod(2)]. Accordingly, if k is an odd integer $\mathcal{R}_2(k) \equiv 1$, and for k an even integer $\mathcal{R}_2(k) \equiv 0$. With this definition we have, for an arbitrary integer k,

$$\delta p_n^{(k)} = \frac{\lambda_u^{(1)}}{D^{(1)}} [-D^{(2)}\delta p_{n-1}^{(k)} + \lambda_u^{(2)} [-D^{(1)}\delta p_{n-2}^{(k)} + \lambda_u^{(1)} [-D^{(2)}\delta p_{n-3}^{(k)} + \lambda_u^{(2)} [\cdots + \lambda_u^{[\mathcal{R}_2(k-1)+1]} [- D^{[\mathcal{R}_2(k)+1]}\delta p_{n-k}^{(k)} + \lambda_u^{[\mathcal{R}_2(k)+1]}\, \boldsymbol{f}_u^{[\mathcal{R}_2(k)+1]} \cdot [\boldsymbol{\xi}_{n-k} - \boldsymbol{\xi}_F^{[\mathcal{R}_2(k)+1]}(p_0)]] \cdots]]]], \tag{3.6a}$$

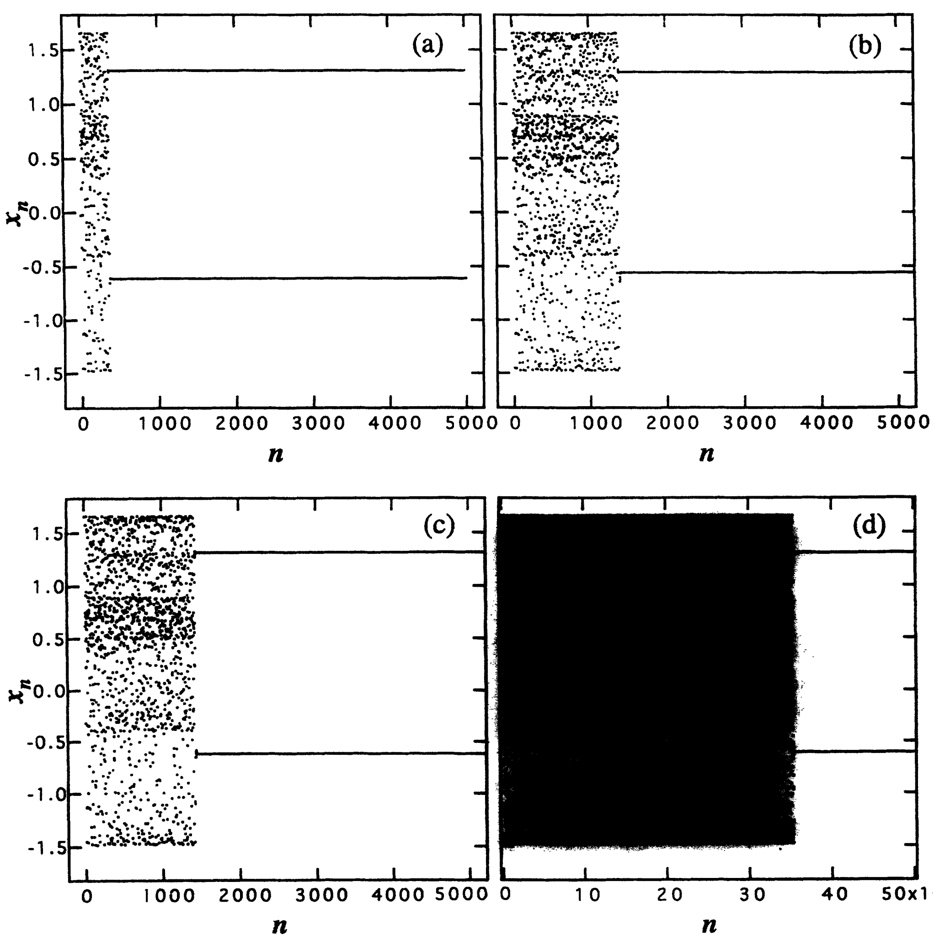

FIG. 6. Controlling the unstable period-two orbit of the Hénon map using the PIC algorithm Eq. (3.6), for k iterates back: (a) $k = 0$, (b) $k = 1$, (c) $k = 5$, and (d) $k = 6$. Note that $k = 0$ corresponds to the OGY formulas Eqs. (3.3) and (3.4).

$$\delta p_{n+1}^{(k)} = \frac{\lambda_u^{(2)}}{D^{(2)}} [- D^{(1)} \delta p_n^{(k)} + \lambda_u^{(1)} [- D^{(2)} \delta p_{n-1}^{(k)} + \lambda_u^{(2)} [-D^{(1)} \delta p_{n-2}^{(k)} + \lambda_u^{(1)} [\cdots + \lambda_u^{[\mathcal{R}_2(k-2)+1]} [- D^{[\mathcal{R}_2(k-1)+1]} \delta p_{n+1-k}^{(k)} + \lambda_u^{[\mathcal{R}_2(k-1)+1]} \boldsymbol{f}_u^{[\mathcal{R}_2(k-1)+1)} \cdot [\boldsymbol{\xi}_{n+1-k} - \boldsymbol{\xi}_F^{[\mathcal{R}_2(k-1)+1]}(p_0)]] \ldots]]]]. \tag{3.6b}$$

In Fig. 6 we show the application of the PIC formulas Eq. (3.6) to the unstable period two orbits of the Hénon map for $k = \{0, 1, 5, 6\}$. Again we note that for larger values of k, the system takes longer to lock onto the unstable orbit of period two. This reflects the reduction in the size of the region of control by the factor $|\lambda_u|^k$, as discussed in Sec. II.

IV. SUMMARY AND CONCLUSIONS

We have presented an extension of the original Ott-Grebogi-Yorke formula in which information measured at a previous $n-k$ crossing the Poincaré section is used for controlling the unstable periodic orbit at the nth crossing. In this method of prior iterate control the region of control about the unstable fixed point is $|\lambda_u|^k$ times smaller than that corresponding to the standard OGY formula, where λ_u is the largest Lyapunov exponent with magnitude greater than unity. This implies that the PIC algorithm is proportionally less resistant to the effects of noise than the OGY algorithm. However, this fact is compensated by the gain in time of k iterates for which the perturbation necessary to control the unstable periodic orbit is known in advance. This makes the PIC method applicable to systems with a fast natural time scale where one to a few cycles may be needed for the detection, calculation, and implementation of the controlling perturbation.

ACKNOWLEDGMENTS

P.M.A and V.K. would like to thank the National Research Council for supporting this work.

APPENDIX A: PRIOR ITERATE CONTROL FOR THE DRESSLER NITSCHE FORMULA

As pointed out by Dressler and Nitsche [9], the transformation from a state vector of phase space variables for the dynamical sytsem to the delay vector constructed from a single time series leads to a map of the form $\boldsymbol{\xi}_{n+1} = \boldsymbol{F}(\boldsymbol{\xi}_n, p_{n-1}, p_n)$. This leads to a linearized map about the fixed point $\boldsymbol{\xi}_F(p_0)$ given by

$$\delta\boldsymbol{\xi}_{n+1} = \boldsymbol{A}\,\delta\boldsymbol{\xi}_n + \boldsymbol{u}\,\delta p_n + \boldsymbol{v}\,\delta p_{n-1}, \tag{A1}$$

where $\delta\boldsymbol{\xi}_n \equiv \boldsymbol{\xi}_n - \boldsymbol{\xi}_F(p_0)$, $\boldsymbol{A} \equiv \boldsymbol{D}_{\boldsymbol{\xi}} \boldsymbol{F}(\boldsymbol{\xi}_F(p_0), p_0, p_0)$, $\boldsymbol{u} \equiv \boldsymbol{D}_{p_n} \boldsymbol{F}(\boldsymbol{\xi}_F(p_0), p_0, p_0)$, and $\boldsymbol{v} \equiv \boldsymbol{D}_{p_{n-1}} \boldsymbol{F}(\boldsymbol{\xi}_F(p_0), p_0, p_0)$. To avoid the possibility of a singular denominator in the formula for the perturbation δp_n, the authors required that $\boldsymbol{f}_u \cdot \delta\boldsymbol{\xi}_{n+2} = 0$ and $\delta p_{n+1} = 0$. This produces the formula [9]

$$\delta p_n = -\lambda_u \left(\frac{\lambda_u}{\lambda_u \boldsymbol{f}_u \cdot \boldsymbol{u} + \boldsymbol{f}_u \cdot \boldsymbol{v}} \boldsymbol{f}_u \cdot \delta\boldsymbol{\xi}_n + \frac{\boldsymbol{f}_u \cdot \boldsymbol{v}}{\lambda_u \boldsymbol{f}_u \cdot \boldsymbol{u} + \boldsymbol{f}_u \cdot \boldsymbol{v}} \delta p_{n-1} \right). \tag{A2}$$

The PIC formula corresponding to Eq. (A2) follows a derivation exactly analogous to Eq. (2.3). Shifting the indices of Eq. (A1) from $n \to n-1$ yields $\delta\boldsymbol{\xi}_n = \boldsymbol{A}\,\delta\boldsymbol{\xi}_{n-1} + \boldsymbol{u}\,\delta p_{n-1} + \boldsymbol{v}\,\delta p_{n-2}$, which is then substituted back into Eq. (A1). As in [9] we require that $\boldsymbol{f}_u \cdot \delta\boldsymbol{\xi}_{n+2} = 0$ and $\delta p_{n+1} = 0$. This yields the following PIC formula:

$$\delta p_n = -\lambda_u \left[\lambda_u \left(\frac{\lambda_u}{\lambda_u \boldsymbol{f}_u \cdot \boldsymbol{u} + \boldsymbol{f}_u \cdot \boldsymbol{v}} \boldsymbol{f}_u \cdot \delta\boldsymbol{\xi}_{n-1} + \frac{\boldsymbol{f}_u \cdot \boldsymbol{v}}{\lambda_u \boldsymbol{f}_u \cdot \boldsymbol{u} + \boldsymbol{f}_u \cdot \boldsymbol{v}} \delta p_{n-2} \right) + \delta p_{n-1} \right]. \tag{A3}$$

The first two terms of Eq. (A3) inside the large square brackets are just the negative of the Dressler-Nistsche formula Eq. (A2) with the indices shifted from $n \to n-1$. Thus analogous to Eq. (2.3), when $\delta p_n = 0$, the terms inside the square brackets simply reproduce the Dressler-Nitsche formula one iterate back. Therefore, instead of using the data $\{\delta\boldsymbol{\xi}_n, \delta p_{n-1}\}$ to control the nth peak, the PIC formula Eq. (A3) uses the information $\{\delta\boldsymbol{\xi}_{n-1}, \delta p_{n-2}, \delta p_{n-1}\}$, one iterate back, to accomplish the same task. The extra factor of λ_u out front implies that the control region for the PIC formula is $|\lambda_u|$ times smaller than the corresponding region when Eq. (A2) is used. A formula analogous to Eq. (2.4) but having the form of Eq. (A3) can be derived for controlling the $n+1$ peak with information from k iterates earlier.

APPENDIX B: THE OGY FORMULA AND CONTROL THEORY

1. The problem of pole placement

As is well known, the OGY control formula for stabilizing an unstable periodic orbit can be derived in just a few short lines. Given a map $\boldsymbol{\xi}_{n+1} = \boldsymbol{F}(\boldsymbol{\xi}_n, p)$, Taylor expand about the unstable fixed point $\boldsymbol{\xi}_F(p_0)$ to obtain the linearized map

$$\delta\boldsymbol{\xi}_{n+1} = \boldsymbol{A}\,\delta\boldsymbol{\xi}_n + \boldsymbol{B}\,\delta p_n, \tag{B1}$$

where $\delta\boldsymbol{\xi}_n \equiv \boldsymbol{\xi}_n - \boldsymbol{\xi}_F(p_0)$, $\boldsymbol{A} \equiv \boldsymbol{D}_{\boldsymbol{\xi}} \boldsymbol{F}(\boldsymbol{\xi}_F(p_0), p_0)$ (called $\boldsymbol{M}$ in Secs. II and III above), and $\boldsymbol{B} \equiv \boldsymbol{D}_p \boldsymbol{F}(\boldsymbol{\xi}_F(p_0), p_0)$. By requiring that $\delta\boldsymbol{\xi}_{n+1}$ has no projection on the unstable manifold, i.e., $\boldsymbol{f}_u \cdot \delta\boldsymbol{\xi}_{n+1} = 0$, we easily obtain

$$\delta p_n = -\frac{\boldsymbol{f}_u \cdot \boldsymbol{A} \cdot \delta \boldsymbol{\xi}_n}{\boldsymbol{f}_u \cdot \boldsymbol{B}}. \tag{B2}$$

This can be brought into the form of Eq. (2.2) by noting that $\boldsymbol{f}_u \cdot \boldsymbol{A} = \lambda_u \boldsymbol{f}_u$ and $\boldsymbol{\Delta} \equiv \partial \boldsymbol{\xi}_F/\partial p = \partial \boldsymbol{F}(\boldsymbol{\xi}_F(p), p)/\partial p = \boldsymbol{A} \cdot \boldsymbol{\Delta} + \boldsymbol{B}$. Therefore $\boldsymbol{f}_u \cdot \boldsymbol{B} = \boldsymbol{f}_u \cdot (1 - \boldsymbol{A}) \cdot \boldsymbol{\Delta} = (1 - \lambda_u)\boldsymbol{f}_u \cdot \boldsymbol{\Delta}$. The procedure of linearizing the map about the fixed point is standard in control theory. The novel feature of the OGY scheme was the author's observation that one could apply control theory techniques about any member of the set of unstable fixed points, which are dense in the attractor when the system is chaotic. Since the chaotic system is essentially ergodic, the system will eventually pass within a neighborhood of the fixed point for which the control algorithm can stabilize the trajectory.

The conventional control theory aspect of the OGY scheme is to pick the perturbation δp in such a way that eigenvalues of $\boldsymbol{A}$ are apppropriately altered. When the system is chaotic, at least one eigenvalue of $\boldsymbol{A}$ has magnitude greater than unity. Thus the perturbation must be chosen in such a way as to make these unstable eigenvalues have magnitude less than one. Choosing $\delta p_n = -\boldsymbol{K}^T \cdot \delta \boldsymbol{\xi}_n$, where $\boldsymbol{K}^T$ is a row vector of unkowns, Eq. (B1) becomes

$$\delta \boldsymbol{\xi}_{n+1} = (\boldsymbol{A} - \boldsymbol{B}\,\boldsymbol{K}^T) \cdot \delta \boldsymbol{\xi}_n. \tag{B3}$$

The problem then translates into solving for the $\boldsymbol{K}^T$ such that the matrix $\boldsymbol{A} - \boldsymbol{B}\,\boldsymbol{K}^T$ has only stable eigenvalues.

In control theory this is known as the *problem of pole placement* and has a unique solution for a predetermined choice of the "regulator poles" (stable eigenvalues) if the $n \times n$ *controlability matrix* $\boldsymbol{C} = (\boldsymbol{B}|\boldsymbol{A} \cdot \boldsymbol{B}| \ldots |\boldsymbol{A}^{n-1} \cdot \boldsymbol{B})$ has rank n. The solution of the pole placement is given [4] by $\boldsymbol{K}^T = (\alpha_n - a_n, \ldots, \alpha_1 - a_1) \cdot \boldsymbol{T}^{-1}$, where $\boldsymbol{T} = \boldsymbol{C}\boldsymbol{W}$, and

$$\boldsymbol{W} = \begin{pmatrix} a_{n-1} & a_{n-2} & \cdots & a_1 & 1 \\ a_{n-2} & a_{n-3} & \cdots & 1 & 0 \\ \vdots & \vdots & \ddots & \vdots & \vdots \\ a_1 & 1 & \cdots & 0 & 0 \\ 1 & 0 & \cdots & 0 & 0 \end{pmatrix}.$$

In the above the $\{a_1, \ldots, a_n\}$ are the coefficients of the characteristic polynomial of $\boldsymbol{A}$,

$$|\lambda \boldsymbol{I} - \boldsymbol{A}| = \lambda^n + a_1 \lambda^{n-1} + \cdots + a_n.$$

For a choice of regulator poles $\{\mu_1, \ldots, \mu_n\}$, the $\{\alpha_1, \ldots, \alpha_n\}$ are the coefficients of the characteristic polynomial of $\boldsymbol{A} - \boldsymbol{B}\boldsymbol{K}^T$,

$$\prod_{i=1}^{n} (\lambda_i - \mu_i) = \lambda^n + \alpha_1 \lambda^{n-1} + \cdots + \alpha_n.$$

2. Examples

For n small, the above computation can be carried out directly by writing down the characteristic polynomial of $\boldsymbol{A} - \boldsymbol{B}\boldsymbol{K}^T$ involving $\{K_1, \ldots, K_n\}$ and choosing them appropriately to give the desired poles. In the following we assume a general two-dimensional map with one stable and one unstable eigenvalue $|\lambda_u| > 1$ and $|\lambda_s| < 1$, respectively. This allows us to write $\boldsymbol{A} = \lambda_s \boldsymbol{e}_s \boldsymbol{f}_s + \lambda_u \boldsymbol{e}_u \boldsymbol{f}_u$. The examples below interpret the OGY and PIC formulas Eqs. (2.2) and (2.3) in terms of a specific choice for the pole placement problem.

a. The OGY formula

Writing $\boldsymbol{B} = B_u \boldsymbol{e}_u + B_s \boldsymbol{e}_s$ and $\boldsymbol{K}^T = K_u \boldsymbol{f}_u + K_s \boldsymbol{f}_s$, the matrix $\lambda \boldsymbol{I} - (\boldsymbol{A} - \boldsymbol{B}\boldsymbol{K}^T)$ becomes

$$\lambda \boldsymbol{I} - (\boldsymbol{A} - \boldsymbol{B}\boldsymbol{K}^T) = \begin{pmatrix} \lambda - \lambda_u + B_u K_u & B_u K_s \\ B_s K_u & \lambda - \lambda_s + B_s K_s \end{pmatrix}.$$

Since we only need to alter the unstable eigenvalue, one possible pole placement solution is obtained by setting $K_s = 0$. The secular equation is then $(\lambda - \lambda_s)(\lambda - \lambda_u + B_u K_u) = 0$. By choosing $K_u = \lambda_u / B_u$ [i.e., $\boldsymbol{K}^T = \lambda_u \boldsymbol{f}_u / (\boldsymbol{f}_u \cdot \boldsymbol{B})$] the matrix $\boldsymbol{A} - \boldsymbol{B}\boldsymbol{K}^T$ is arranged to have eigenvalues $\lambda = \{\lambda_s, 0\}$ and so is rendered stable. The perturbation is then given by $\delta p_n = -\boldsymbol{K}^T \cdot \delta \boldsymbol{\xi}_n = -\lambda_u (\boldsymbol{f}_u \cdot \delta \boldsymbol{\xi}_n)/(\boldsymbol{f}_u \cdot \boldsymbol{B})$, which is just the OGY solution Eq. (B2). Thus the OGY formula is that particular solution of the pole placement problem which sets $\lambda_u \to 0$ and leaves λ_s unaltered. For higher-dimensional maps, this generalizes to having all unstable eigenvalues of $\boldsymbol{A}$ beign set to zero and leaving all the stable eigenvalues unaltered. Clearly this is not the only solution to the pole placement problem since the necessary and sufficient condition to stablize the unstable periodic orbit is for the eigenvalues of $\boldsymbol{A} - \boldsymbol{B}\boldsymbol{K}^T$ to have any value of magnitude less than unity. This latter point accounts for the robustness which is seen in OGY algorithm. In [3] the particular choice of the pole placement solution indicated by the OGY formula is shown to be optimal in that it minimizes the average time during which the orbit wanders chaotically before it can be stabilized.

b. The PIC formula

We consider now the PIC formula for one iteration back Eq. (2.3). In addition to Eq. (B1), we write the perturbation as $\delta p_n^{(1)} = -\boldsymbol{K}^T \cdot \delta \boldsymbol{\xi}_{n-1} - k\, \delta p_{n-1}^{(1)}$. Defining

$$\delta \tilde{\boldsymbol{\xi}}_n = \begin{pmatrix} \delta \boldsymbol{\xi}_n \\ \delta p_n \end{pmatrix}, \qquad \tilde{\boldsymbol{A}} = \begin{pmatrix} \boldsymbol{A} & \boldsymbol{B} \\ \boldsymbol{0} & 0 \end{pmatrix},$$

$$\tilde{\boldsymbol{B}} = \begin{pmatrix} \boldsymbol{0} \\ 1 \end{pmatrix}, \qquad \tilde{\boldsymbol{K}} = \begin{pmatrix} \boldsymbol{K} \\ k \end{pmatrix},$$

we then have the control problem

$$\delta \tilde{\boldsymbol{\xi}}_{n+1} = (\tilde{\boldsymbol{A}} - \tilde{\boldsymbol{B}}\tilde{\boldsymbol{K}}^T) \cdot \delta \tilde{\boldsymbol{\xi}}_n. \tag{B4}$$

As in the preceding section, setting $K_s = 0$ yields the secular equation $(\lambda - \lambda_s)[(\lambda - \lambda_u)(\lambda + k) + B_u K_u] = 0$. We obtain Eq. (2.3) by choosing $k = \lambda_u$ and $K_u =$

λ_u^2/B_u. Since it was derived from the OGY formula, we see that the PIC formula Eq. (2.3) is again that solution of the pole placement problem for which the unstable eigenvalues of $\boldsymbol{A}$ are set to zero and the stable eigenvalues are left unaltered.

This above result is true in addition for the PIC formula for $\delta p_n^{(k)}$ for arbitrary k, Eq. (2.4). This involves defining additional variables in order to define a composite state vector $\delta\tilde{\boldsymbol{\xi}}_n$ in analogy with the above example. For example, for the PIC case $k = 2$ one has $\delta\boldsymbol{\xi}_{n+1}$, given by Eq. (B1), and $\delta p_n^{(2)} = -\boldsymbol{K}^T \cdot \delta\boldsymbol{\eta}_{n-1} - k_1\,\delta p_{n-1}^{(2)} - k_2\,\delta q_{n-1}^{(2)}$, where we have introduced the new variables $\delta\boldsymbol{\eta}_n = \delta\boldsymbol{\xi}_{n-1}$ and $\delta q_n^{(2)} = \delta p_{n-1}^{(2)}$. The control problem has the form of Eq. (B4) where the composite state vector is given by $\delta\tilde{\boldsymbol{\xi}}_n = \{\delta\boldsymbol{\xi}_n, \delta p_n^{(2)}, \delta\boldsymbol{\eta}_n, \delta q_n^{(2)}\}$. In general, if the controllability maxtrix formed from $\tilde{\boldsymbol{A}}$ and $\tilde{\boldsymbol{B}}$ has rank n, then the control problem yields a solution. This is the case for PIC for arbitrary k, and formula Eq. (2.4) is that particular choice of solution for which the unstable eigenvalues of $\boldsymbol{A}$ are set to zero and the stable eigenvalues are left unaltered.

[1] E. Ott, C. Grebogi, and J. A. Yorke, Phys. Rev. Lett. **64**, 1196 (1990).

[2] T. Shinbrot, E. Ott, C. Grebogi, and J. Yorke, Nature **363**, 411 (1993); T. Shinbrot, Nonlin. Sci. Today **3**, 1 (1993).

[3] F.J. Romerias, C. Grebogi, E. Ott, and W.P. Dayawansa, Physica D **58**, 165 (1992).

[4] K. Ogata, *Control Engineering*, 2nd ed. (Prentice-Hall, Englewood Cliffs, NJ, 1990), Chap. 10, pp. 772–889; for applications to controlling chaos and an explicit example involving the Hénon map, see [3] and [5].

[5] E. Ott, *Chaos in Dynamical Systems* (Cambridge University Press, New York, 1993), pp. 145–148.

[6] E. Ott, C. Grebogi, and J.A. Yorke, in *Chaos: Soviet-American Perspectives on Nonlinear Science*, edited by D.K. Campbell (AIP, New York, 1990), p. 153.

[7] E.R. Hunt, Phys. Rev. Lett. **67**, 1953 (1991).

[8] R. Roy, T.W. Murphy, T.D. Maier, Z. Gillis, and E.R. Hunt, Phys. Rev. Lett. **68**, 1259 (1992).

[9] U. Dressler and G. Nitsche, Phy. Rev. Lett. **68**, 1 (1992); Physica D **58**, 153 (1992).

[10] V. Petrov, B. Peng, and K. Showalter, J. Chem. Phys. **96**, 7506 (1992).

[11] R.W. Rollins, P. Parmananda, and P. Shepard, Phys. Rev. E **47**, R780 (1993).

[12] D. Auerbach, E. Ott, C. Grebogi, and J. A. Yorke, Phys. Rev. Lett. **69**, 3479 (1992).

[13] A. Gavrielides, V. Kovanis, and P.M. Alsing, Chaos in Optics [Proc. SPIE **2039**, 250 (1993)]; P. M. Alsing, A. Gavrielides, and V. Kovanis, Phys. Rev. E **49**, 1225 (1994).

[14] I.B. Schwartz and I. Triandaf, Phys. Rev. A **46**, 7439 (1992).

[15] Z. Gills, C. Iwata, R. Roy, I.B. Schwartz, and I. Triandaf, Phys. Rev. Lett. **69**, 3169 (1992).

[16] S. Bielawski, D. Derozier, and P. Glorieux, Phys. Rev. E **49**, R971 (1994); Phys. Rev. A **47**, R2492 (1993).

[17] N.J. Mehta and R.M. Henderson, Phys. Rev. A **44**, 4861 (1991).

[18] P.M. Alsing, A. Gavrielides, and V. Kovanis, Phys. Rev. E. **49**, 1225 (1994); Chaos/Nonlinear Dynamics: Methods and Commercialization [Proc. SPIE **2037**, 126 (1993)]; in these papers it was shown that the neural network could learn and implement the one-iterate back PIC control formula.

[19] K. Pyragas, Phys. Lett. A **170**, 421 (1992); **181**, 203 (1993); K. Pyragas and A. Tamaševičius, *ibid.* **180**, 99 (1993).

[20] J.E. Socolar, D.W. Sukow, and D.J. Gauthier, Phys. Rev. E (to be published); D.J. Gauthier, D.W. Sukow, H.M. Concannon, and J.E. Socolar Phys. Rev. E **50**, 2343 (1994).

[21] P. So, E. Ott, and W.P. Dayawansa, Phys. Lett. A **176**, 421 (1993); Phys. Rev. E **49**, 2650 (1994).

[22] W.L. Ditto, S.N. Rauseo, and M.L. Spano, Phys. Rev. Lett. **65**, 3211 (1990).

[23] J.S. Sacher, D. Baums, P. Pankin, W. Elsässer, and E.O. Göbel, Phys. Rev. A **45**, 1893 (1992).

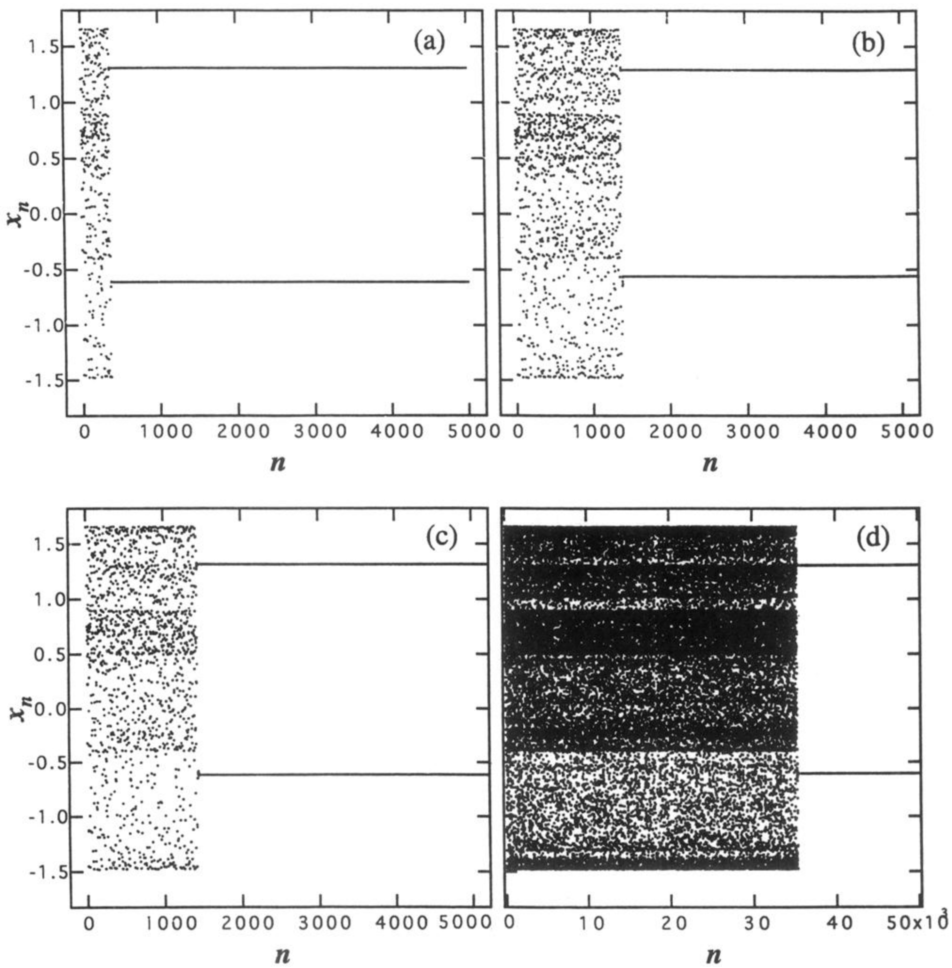

FIG. 6. Controlling the unstable period-two orbit of the Hénon map using the PIC algorithm Eq. (3.6), for k iterates back: (a) $k = 0$, (b) $k = 1$, (c) $k = 5$, and (d) $k = 6$. Note that $k = 0$ corresponds to the OGY formulas Eqs. (3.3) and (3.4).